Material Screening for Gas Sensing using an Electronic Nose: Gas Sorption Thermodynamic and Kinetic Considerations

Ashwin Kumar Rajagopalan* and Camille Petit*

Department of Chemical Engineering, Imperial College London, London, SW7 2AZ, United Kingdom

E-mail: a.rajagopalan@imperial.ac.uk; camille.petit@imperial.ac.uk

Abstract

To detect multiple gases in a mixture, one must employ an electronic nose or sensor array, composed of several materials as a single material cannot resolve all the gases in a mixture accurately. Given the many candidate materials, choosing the right combination of materials to be used in an array is a challenging task. In a sensor whose sensing mechanism depends on a change in mass upon gas adsorption, both the equilibrium and kinetic characteristics of the gas-material system dictate the performance of the array. The overarching goal of this work is two-fold. First, we aim to highlight the impact of thermodynamic characteristics of gas-material combination on array performance and to develop a graphical approach to rapidly screen materials. Second, we aim to highlight the need to incorporate the gas sorption kinetic characteristics to provide an accurate picture of the performance of a sensor array. To address these goals, we have developed a computational test bench that incorporates a sensor model and a gas composition estimator. To provide a generic study, we have chosen, as candidate materials, hypothetical materials that exhibit equilibrium characteristics similar

to metal organic frameworks (MOFs). Our computational studies led to key learnings, namely: (1) exploit the shape of the sensor response as a function of gas composition for material screening purposes for gravimetric arrays; (2) incorporate both equilibrium and kinetics for gas composition estimation in a dynamic system; and (3) engineer the array by accounting for the kinetics of the materials, the feed gas flow rate, and the size of the device.

1 Introduction

The global gas sensor market has been expanding rapidly over the years due to the increased use of sensors in industrial, medical, and automotive sectors.[1] Major focus has been on sensing carbon dioxide (CO_2), methane (CH_4), water vapor (H_2O), nitrogen oxides (NO_x), and volatile organic compounds (VOCs), most of which constitute greenhouse gases (GHG). Gas sensing devices can be classified into methods that rely on electrical variation and methods that rely on other property changes. The former group encompasses impedance sensors, chemicapacitive sensors, chemiresistive sensors, and electrochemical sensors.[2] The latter group encompasses optical sensors (absorption/transmission spectroscopy sensor, photo ionization detector sensor, luminescence sensor), gravimetric sensors (quartz crystal microbalance (QCM) sensors, surface acoustic wave (SAW) sensors, microcantilever sensors), and acoustic sensors.[2–8] The most important characteristics for any gas sensor are its selectivity , chemical and thermal stability, sensitivity, reusability, and response time. Apart from these, factors like portability, cost, and energy requirement to operate the sensor can play a role in the suitability and application of a particular sensor. The active sensing component of most commercial sensors are either organic-polymers or inorganic-metal oxides. They exploit some form of electrical variation for monitoring the change, which requires the active sensitive material to exhibit electrical conductivity. Polymeric sensors often suffer from poor selectivity and poor long term stability.[2,9] Metal oxide sensors must be usually operated at temperatures exceeding 200 °C. This unfavorable feature hinders their usage for

ambient temperature gas sensing. These sensors also exhibit high cross-selectivity in the presence of multiple gases.[2,3,9]

Porous materials like zeolites and metal-organic frameworks (MOFs) have shown great promise for gas storage and separation processes.[10–12] This is largely attributed to the ability to tune their structure, composed of metallic ions or clusters and organic linkers, which leads to an infinite number of possible structures. Due to these features, MOFs can exhibit a high selectivity toward a desired target gas. MOFs have been used as active sensing materials to detect vapors and VOCs,[13–19] water vapor,[20,21] CO_2,[9,22,23] O_2,[24] and sulfur containing gases[25,26] (SO_2 and H_2S). A priori, MOFs are suitable candidates for active sensing material owing to their tunable selectivity toward a target gas, ability to be coated onto miniature sensors, and ability to function under both room and elevated temperatures. Yet, the focus of research so far has been on either sensing of or increasing the selectivity for a particular gas. Quantification of a wide range of gases has not been proven. The integration of MOF into actual sensor devices is even less explored. In short, although very promising, the development of MOF-based portable gas sensors is at its infancy and several technical challenges related to their implementation remain to be overcome.

Gravimetric sensors provide an excellent platform for gas sensing due to their simple miniature construction, commercial availability, low cost, and ability to provide online data.[8,27,28] In these sensors the gas uptake, on an active sensing surface (porous materials, e.g. MOFs), is inferred by changes in physical quantities like resonance frequency (for QCM) or modulation of surface acoustic waves (for SAW). The mass detection limit of these devices are usually in the order of nanograms.[4,5,8] As explained previously, MOFs show a great potential for gas sensing applications and can be used in a gravimetric sensor.[29] Yet, a single *magic* MOF material can hardly ever be used to detect multiple gases in a gas stream. An array of sensors (also known as *electronic nose*, analogous to human olfactory system) has been proposed to overcome the issue of multigas sensing.[15,30–35] An array of sensor is composed of multiple sensor elements coated with different materials exhibiting varying se-

lectivity toward a particular gas. There exists only a handful of experimental studies of such an array using MOFs.[15,36]

Given the large number of experimental and hypothetical MOFs reported in the literature, there is a necessity to select materials from the 1000s of possible candidates in a smart fashion that guarantees excellent sensing performance in a sensor array. To this aim, Wilmer and coworkers and Simon and coworkers have recently provided excellent screening frameworks.[37–42] The former comprises of computational studies aimed at providing a probabilistic metric to quantify sensing performance of an array and at efficiently screening several materials using an evolutionary optimization algorithm for CH_4 and CO_2 sensing. The latter comprises of computational studies aimed at using elegant mathematical concepts to screen materials under dilute conditions for a two- and three-gas system and to evaluate the fitness of combinations of materials in a sensor array for a two-gas system.

The overarching goal of this work is two-fold. We aim to systematically highlight the impact of thermodynamics of the gas-material system on gas sensing and to provide a simple graphical approach to screen porous materials that can be used in a gravimetric sensor. This aspect would be an addition to what was covered in the aforementioned computational studies. Once the equilibrium characteristics of a material is available, the graphical approach would provide a quick check to determine whether the material will be a suitable candidate for a given gas sensing application. If the material is not a suitable candidate, the same approach can be used to mix and match different materials to get a good sensing accuracy. Given the sheer number of MOFs reported in the literature, a simple tool like the one proposed in this work can be handy. This approach relies only on the thermodynamics of the system and is aimed to be qualitative. For a more rigorous approach, the computational studies from the previous subsection can be used.[38,41] The second goal of our study is to systematically highlight the importance of incorporating adsorption kinetics for gravimetric sensors in the screening process. The computational studies from the previous subsection were all performed under equilibrium conditions. However, adsorption is driven by both

equilibrium and kinetics. Within the context of gas sensing, the amount of gas adsorbed will determine the changes in the sensor response and the kinetics will determine the sensor response time. The kinetic aspects of gas sensing have often been overlooked and not been studied in detail. Our work does not pertain to any specific mixture(s) of gas. The methodology, results, and conclusions from this study can be easily transferred to any gravimetric sensor with porous materials as active sensing surface.

The article is organized as follows. In Section 2, we give an overview of the modeling framework used in this study. In Section 3, we present cases studies on the impact of thermodynamics and the graphical approach to screen porous materials. In Section 4, we highlight the importance of incorporating kinetic models on gas sensing. Finally, in Section 5, we summarize the key outcomes and share thoughts on the way forward.

2 Methodology

The studies presented in this work are purely computational in nature. A simple schematic of the problem statement and the workflow of the computational test bench developed in this work is shown in Figure 1. This test bench is comprised of two components, namely, a sensor array simulator and a composition estimator. The former serves as a proxy to an experimental sensor array and provides what we refer to as the 'true' (or experimental) sensor response. In this work, the sensor response is equivalent to the amount of gas adsorbed on the active sensing surface (i.e., the porous material). Upon the availability of the amount of gas adsorbed, the composition estimator provides the composition of the gas that was exposed to the porous material that led to the given sensor response. These two components of the computational test bench are discussed in the following subsections.

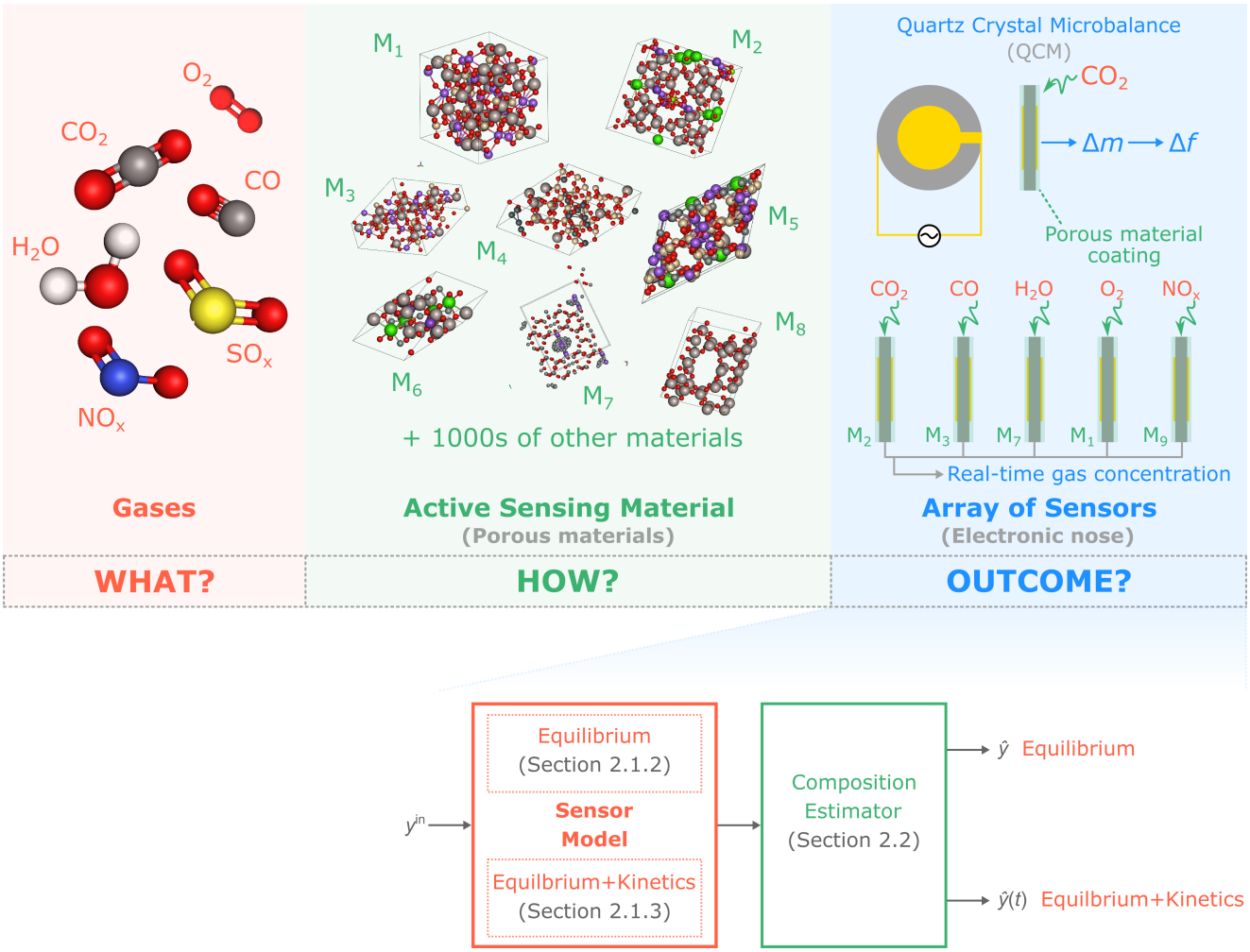

Figure 1: A visual schematic of the problem addressed in this work. The problem tackled here is the real-time quantitative sensing of gases (WHAT?) using an array of sensors/electronic nose (OUTCOME?) with porous materials (M_i) as the active sensing material (HOW?). The schematic here indicates a Quartz Crystal Microbalance (QCM) based transduction mechanism. However, this could be any other technique based on gravimetry. The bottom panel indicates the workflow of the computational test bench developed in this work that incorporates a sensor model (either incorporating pure equilibrium or combined equilibrium and kinetics) and the composition estimator. The input to the test bench is the real gas composition y^{in} to be sensed and the output is the estimated gas composition $\hat{y}$.

2.1 Sensor Array Simulator

To simulate the sensor array, it is necessary to first identify the gases that will be sensed and the materials that will form the array. Subsequently, the thermodynamics (i.e. adsorption equilibria) and the kinetics of the gas-material combination must be defined. If the kinetics are not considered, the sensor response can be obtained by estimating the gas uptake in a

given material at a given partial pressure (i.e. composition). If kinetics are considered, the thermodynamics of the system is coupled with the kinetics. This is done by integrating the mass balance equations for the gas and the solid phases that define the evolution of the gas uptake of the sensor array as function of time. The following subsections provide details regarding how these cases are handled in the computational framework.

2.1.1 Definition of the Gas-Material System

To keep the study as general as possible, we consider hypothetical materials instead of real materials. The equilibrium properties of these materials are chosen such that their adsorption capacities and heats of adsorption resemble the ones of common porous materials (e.g. MOFs, Zeolites). The adsorption equilibria of these materials are defined using the single-site Langmuir isotherm (a Type I isotherm). Further, the competition between the gases is defined using the extended single-site Langmuir isotherm, retaining the parameters of the pure gases, as follows

$$\begin{aligned} q_j^*(P,T,y_j) &= \frac{q_{\mathrm{sat},j} b_j c_j}{1+\sum_{k=1}^{g} b_k c_k} \\ b_j &= b_{0,j}\exp\left(-\frac{\Delta U_j}{RT}\right) \\ c_j &= \frac{P y_j}{RT} \end{aligned} \tag{1}$$

where q_j^* [$\mathrm{mol\,m^{-3}}$] is the equilibrium adsorption capacity of gas j at pressure P [Pa] and temperature T [K], $q_{\mathrm{sat},j}$ [$\mathrm{mol\,m^{-3}}$] is the saturation adsorption capacity, c_j is the concentration of the gas, y_j [-] is the corresponding mole fraction, g is the total number of gases in the mixture, b_j is the temperature dependent adsorption equilibrium constant, and ΔU_j [$\mathrm{J\,mol^{-1}}$] is the internal energy.

For a two-gas system, the molecular weights of these gases are $\mathbf{M}$ [$\mathrm{g\,mol^{-1}}$] = [44.01 28.01].

For the three-gas system, the corresponding molecular weights are $\mathbf{M} = [44.01\ 28.01\ 15.99]$. All the simulations are performed at a temperature of 298.15 K and a pressure of 1 bar. Depending on the system being studied, the molecular weights, temperature, and pressure can be changed in the computational framework.

2.1.2 Sensor Response: Accounting for only Thermodynamics

In the absence of kinetics or estimating the gas composition at equilibrium conditions, the response m_i of a gravimetric sensor (e.g. QCM) coated with material i at pressure P and temperature T exposed to a gas mixture of composition $\mathbf{y}$ is given as

$$m_i(P, T, \mathbf{y}) = \sum_{j=1}^{g} \rho_i q_j^*(P, T, y_j) M_j \qquad i \in [1, n] \tag{2}$$

where ρ_i [kg m^{-3}] is the density of material i, $q_j^*(P, T, y_j)$ is the equilibrium adsorption capacity, obtained from eq 1, and M_j is the molecular weight of the gas j. The sensor response takes the above form because the gravimetric sensor can only detect the total change in the mass and cannot identify the individual contribution of the constituent gases to the total mass uptake. If a sensor array/electronic nose, with more than one material, is used, the sensor response of a number of materials (n) will be used to determine the gas composition.

2.1.3 Sensor Response: Accounting for Both Thermodynamics and Kinetics

When accounting for kinetics, a detailed mathematical model that incorporates the resistance offered by a porous material to adsorb a given gas must be considered. This mathematical model must describe the evolution of the mass uptake over time by coupling the thermodynamics and kinetics of the porous material. The adsorption capacity and the kinetics of the gas on a given material constitute the so-called *material constraints*. In practice, if one uses a QCM or a SAW sensor, additional constraints exist e.g. the maximum allowable flow rate of the gas to be sensed, the mass/volume of the active sensing material coated on the sensor, and the unavoidable dead volume of the device. These factors constitute the so-called

engineering constraints.

Based on the above considerations, we formulate a mathematical model for the sensor coated with a given material. To this aim, we assume the combined sensor and the material system to be a perfectly mixed cell. This is analogous to a packed bed in chromatography/adsorption when the length of the column tends to zero.[43] Therefore, the component mass balance for the gas j is written as

$$F^{\text{in}} c_j^{\text{in}} - F c_j = V_{\text{g}} \frac{\mathrm{d}c_j}{\mathrm{d}t} + V_{\text{s}} \frac{\mathrm{d}q_j}{\mathrm{d}t} \tag{3}$$

where F^{in} [$\mathrm{m^3\,s^{-1}}$] and F [$\mathrm{m^3\,s^{-1}}$] are the volumetric flow rate of the gas mixture at the inlet and the outlet, respectively, c_j^{in} and c_j are the concentration of the gas j at inlet and outlet, respectively, q_j is the amount of gas adsorbed in the porous material, V_{g}[$\mathrm{m^3}$] is the dead volume of the device, and V_{s} [$\mathrm{m^3}$] is the volume of the porous material coated on the sensor.

We assume the rate of uptake of gas j in the porous material to be described using the linear driving force (LDF) model as

$$\frac{\mathrm{d}q_j}{\mathrm{d}t} = k_j \left(q_j^* - q_j \right) \tag{4}$$

where q_j [$\mathrm{mol\,m^{-3}}$] is the amount of gas adsorbed in the material at time t, q_j^* is the equilibrium adsorption capacity, obtained from eq 1, and k_j [$\mathrm{s^{-1}}$] is the lumped kinetic rate constant for a given gas j that describes the resistance to mass transfer from the gas phase to the solid phase.

Finally, to close the system of equations, we impose a mass conservation constraint using

$$\sum_{j=1}^{g} y_j = 1 \tag{5}$$

Additionally, if the pressure drop in the sensor is assumed to be negligible, there will be

$2g+1$ unknowns, namely the g gas compositions ($\mathbf{y}$), the g solid phase uptakes ($\mathbf{q}$), and the volumetric flow rate at the outlet F. Equations 3 through 5 provides $2g+1$ equations to estimate the $2g+1$ unknowns.

Under the assumption of negligible pressure drop and using the equation of state given in eq 1, eqs 3 through 5 are reformulated as follows

$$\begin{aligned} \frac{\mathrm{d}q_j}{\mathrm{d}t} &= k_j\left(q_j^* - q_j\right) \qquad j \in [1,g] \\ F^{\mathrm{in}}\frac{P}{RT} - F\frac{P}{RT} &= V_{\mathrm{s}}\sum_{j=1}^{g}\frac{\mathrm{d}q_j}{\mathrm{d}t} \\ \frac{\mathrm{d}y_j}{\mathrm{d}t} &= \frac{RT}{PV_{\mathrm{g}}}\left[F^{\mathrm{in}}\frac{Py_j^{\mathrm{in}}}{RT} - F\frac{Py_j}{RT} - V_{\mathrm{s}}\frac{\mathrm{d}q_j}{\mathrm{d}t}\right] \qquad j \in [1,g) \end{aligned} \tag{6}$$

We use a stiff solver in the *solve_ivp* function of the `scipy` package in Python 3.8.5.[44] to integrate the aforementioned set of equations for time span t_{int} [s]. These equations have to be solved for each material that is present in the sensor array. The initial conditions for the aforementioned problem are

$$\begin{aligned} y_j(0) &= 0 \qquad j \in [1,g) \\ q_j(0) &= 0 \qquad j \in [1,g] \\ F(0) &= F^{\mathrm{in}} \end{aligned} \tag{7}$$

When performing simulations considering the kinetics of the system, apart from the gases of interest, an additional non-adsorbing inert gas is introduced. In reality, this will translate to purging the material with an inert gas to prepare the material to sense incoming feed gas.

2.2 Composition Estimator

The estimation of gas composition with the knowledge of the amount adsorbed is the inverse problem to the traditional gas adsorption problem encountered in the porous mate-

rials/adsorption process community, i.e. the gas uptake in a material when exposed to a gas mixture of known concentration. One can compute the gas composition if the uptake is known either by employing a look up table or by framing an optimization problem. In this work, we use the latter approach. An optimization problem is framed that minimizes the error between the "true" measurement $m_{\text{exp},i}$ and the simulated measurement $m_{\text{sim},i}$ obtained by varying the gas composition $\mathbf{y}$. For a sensor array, the error is the sum of the individual contributions from all the materials of the array.

Mathematically, when accounting only for the thermodynamics, the optimization problem takes the following form

$$\begin{aligned} \underset{\mathbf{y}}{\text{minimize}} \quad & \sum_{i=1}^{n} \left(\frac{m_{\text{exp},i} - m_{\text{sim},i}(\mathbf{y})}{m_{\text{exp},i}} \right)^2 \\ \text{subject to} \quad & 0 \leq y_j \leq 1 \qquad j \in [1, g] \\ & \sum_{j=1}^{g} y_j = 1 \end{aligned} \tag{8}$$

where m_{exp} and m_{sim} are obtained using eq 2.

When accounting for both thermodynamics and kinetics, the aforementioned mathematical expression has to be reformulated to incorporate the evolution of the gas uptake. Upon reformulation, the optimization problem takes the following form

$$\begin{aligned} \underset{\mathbf{y}}{\text{minimize}} \quad & \sum_{i=1}^{n} \left(\frac{\mathbf{m}_{\text{exp},i} - \mathbf{m}_{\text{sim},i}(\mathbf{y})}{\mathbf{m}_{\text{exp},i}} \right)^2 \\ \text{subject to} \quad & 0 \leq y_j(t) \leq 1 \qquad j \in [1, g] \\ & \sum_{j=1}^{g} y_j(t) = 1 \end{aligned} \tag{9}$$

where $\mathbf{m}$ is a vector of gas uptake on a material i as a function of time obtained by solving the full model given by eq 6. This expression is equivalent to minimizing the error between the "true" gas uptake profile and the simulated gas uptake profile.

We use the *basinhopping* algorithm of the `scipy` package in Python 3.8.5.[44] to solve the optimization problem. The basin hopping algorithm combines a global stepping algorithm and a local minimization algorithm to ensure that the entire decision variable space ($\mathbf{y}$) is explored. We use a total of 50 iterations in the basin hopping algorithm and the minimum value obtained at the end of these iterations is assumed to be the global minimum.

3 Thermodynamic Considerations

In this section, we discuss the thermodynamic considerations, i.e. the gas uptake in a given material at equilibrium, within the context of gas sensing. Subsequently, we propose a simple graphical method used to provide a quick check on whether a given material or a combination of materials has the potential to resolve accurately the composition of gases being sensed. To this aim, we provide first a simple study that highlights the need to incorporate a combination of materials for good sensing performance (see Section 3.1). Second, we show that even with a combination of materials there is no guarantee that an optimal sensing performance can be obtained without introducing mathematical constraints to estimate the gas composition (see Section 3.1). Third, we demonstrate that even after incorporating the constraint, the ability of the material(s) to resolve the "true" gas composition accurately depends on the shape of the response curve (i.e. total gas uptake vs. partial pressure of the gas) (see Section 3.2). Finally, we propose a simple graphical approach to provide a qualitative region of gas composition where a given material or combination of materials can exhibit good sensing performance (see Section 3.3). This work paves way for a rapid screening of materials for gas sensing. The readers are directed to other works reported in the literature for a more quantitative approach toward material screening[38,39] and for a mathematical understanding of why combination of materials exhibit a given performance.[41,42]

3.1 Need for Combination of Materials

To highlight the need to combine materials with distinct equilibrium characteristics, we conducted a simple case study with 100 hypothetical materials. Subsequently, a sensor array composed of either one or two materials was exposed to a binary test gaseous stream of a known composition $\mathbf{y} = [0.05\ 0.95]$. Based on this known composition, the "experimental" sensor response m_{exp} was computed, using eq 2, for each material in the array. Given this sensor response, the optimization problem set in eq 8 was solved to obtained the estimated composition $\hat{\mathbf{y}}$. This approach serves as a proxy to a real experiment using the array. If the materials in a given sensor array are capable of resolving the gas sensor, then $\hat{\mathbf{y}} = \mathbf{y}$. We considered two different scenarios. One in which the mass conservation constraint, given in eq 8, was not imposed and one in which it was imposed. Ideally, the former should be sufficient if the materials exhibit good sensitivity toward changes in gas phase composition. For example, for a two-gas system, two materials should be sufficient to resolve the gas composition accurately. If not, the constraint posed in the latter case would aid in the computation of the gas compositions by providing an additional physically consistent information on the system. The one- and two-material sensor arrays led to 100 and 4950 unique combinations, respectively, using the 100 hypothetical materials. The composition estimates from these arrays are visualized in Figure 2 in the form of a probability distribution f. We draw two main observations from the results. First, as expected, moving from a sensor array composed of one material to two materials leads to a better resolution of the gas composition as evident by the narrow distribution of compositions around the "true" gas composition. This result highlights the strength of building a sensor array such that the number of materials is at least equal to the number of gases being sensed. Second, the incorporation of the mass conservation constraint (see eq 8) in the optimization routine also leads to a better resolution of the gas composition, even for the sensor array composed of only one material due to the reasons explained above. We exploit this finding in all the studies shown in the following sections by incorporating the mass conservation constraint.

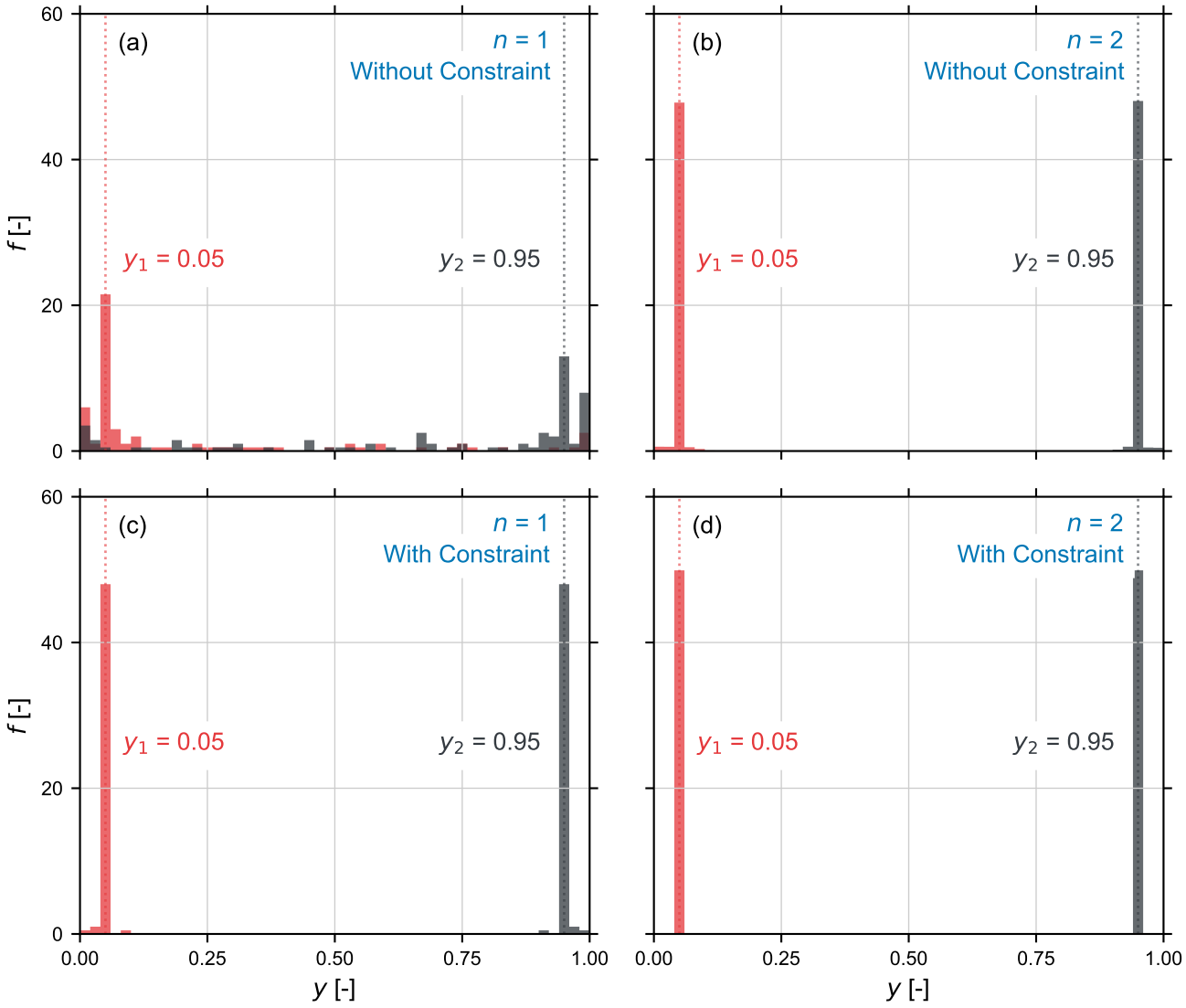

Figure 2: Distribution of estimated gas compositions f, obtained by solving eq 8, for a two-gas system using a sensor array composed of **(a)** one material ($n = 1$) and **(b)** two materials ($n = 2$) without incorporating the mass conservation constraint in the optimization routine. The corresponding distributions accounting for mass conservation constraint for **(c)** one material ($n = 1$) and **(d)** two materials ($n = 2$). The "true" gas composition for gas 1 (red) y_1 is 0.05 and gas 2 (gray) y_2 is 0.95 and they are shown using the dotted vertical lines. A bin size of 0.02 was used for all the distributions. The distributions are normalized so that the area under the curve is one.

3.2 Effect of Shape of Sensor Response

When a sensor array is used in practice, at each time instant, the mass change due to gas adsorption on each material is monitored and the optimization problem defined in eq 8 is

solved to obtain the gas compositions. If this operation is repeated a sufficient number of times, one can obtain a distribution of gas compositions. This distribution will be characterized by its mean $\hat{\mu}$ and standard deviation $\hat{\sigma}$. For a good sensor array, the mean should be as close as possible to the "true" gas composition and the standard deviation should be as small as possible. The former guarantees obtaining the correct gas composition, while the latter guarantees a good sensitivity of the array when subjected to changes in the feed gas composition. In practice, these two quantities depend on the sensor response of the array.

Under strictly equilibrium conditions, the response of a given sensor or sensor array, given by eq 2, is a consequence of the adsorption isotherm of a gas-material combination. To highlight the effect of the shape of the sensor response as a function of the gas composition which derives from the specific gas adsorption patterns, we constructed three hypothetical arrays, each with only one material (A-C). Subsequently, these arrays were exposed to eight different "true" gas compositions (a two-gas mixture). Their composition estimation was repeated a 1000 times to obtain the distribution of gas compositions. The sensor performance was gauged using two metrics, namely, the relative error of the estimated mean gas composition ψ and the coefficient of variation χ. The former is defined as the relative error of mean $\hat{\mu}$ of the estimated distribution with respect to the mean of the "true" gas composition μ. The latter is defined as the ratio of the standard deviation $\hat{\sigma}$ to the mean $\hat{\mu}$ of the estimated distribution.

The equilibrium sensor response m for the three hypothetical sensor arrays as a function of the gas composition y_1 is illustrated in Figure 3a. The three arrays exhibit different adsorption behaviors. For arrays A and C, gas 1 is preferentially adsorbed over gas 2, while for array B, gas 2 is preferentially adsorbed over gas 1. In other words, we observe differences in the shape of the sensor response. Additionally, the sensor response for arrays A and B are extremely nonlinear with respect to the gas composition, while for array B it is closer to being linear. As discussed below, the shape of the response has major implications on estimating the composition accurately.

The relative error of the estimated mean gas composition ψ and the coefficient of variation χ for the three arrays at different gas compositions is shown in Figure 3b and Figure 3c, respectively. Two observations can be made based on the outcome of the simulations. First, array C performs the best over a wide range of gas composition, as indicated by the lower value of ψ and χ over almost the entire range of composition. Second, array A and B exhibit contrasting behaviors in line with the shape of their response. Array A shows higher nonlinearity at lower compositions and therefore has a lower value of ψ and χ at lower gas compositions, while array B has a lower value for both the quantities at higher gas compositions. For array A, when $y_1 > 0.10$, the sensor response barely changes thereby leading to an incorrect mean value and a broader distribution of compositions around the mean. In the next subsection, hypothetical arrays with more than one material will be constructed to mitigate the high errors and further reinforce the observations seen here. If measurement noise is incorporated, the performance of the arrays can change depending on the shape of the response. However, this aspect is not discussed here and the reader is directed toward literature that looks into measurement noise in detail.[38,41,42]

To conclude, based on the above observations, one can easily confirm if a sensor array possesses the ability to resolve a gas mixture accurately at a given gas composition. This approach is beneficial as it can help screen unsuitable candidates at a fraction of computational cost when compared to rigorous screening approaches, which are often time consuming.

3.3 Evaluating Array Performance using the Sensor Response Shape

In the previous subsection, we show that the accuracy in predicting the actual gas composition with little deviation from the mean value depends heavily on the shape of the sensor (material) response. Additionally, a nonlinear sensor response leads to a better accuracy to resolve a gas mixture whose composition falls in the nonlinear region. Based on these two observations, we developed a simple graphical tool to identify regions of gas composition to which a given sensor array will have the best performance in terms of resolving the gas

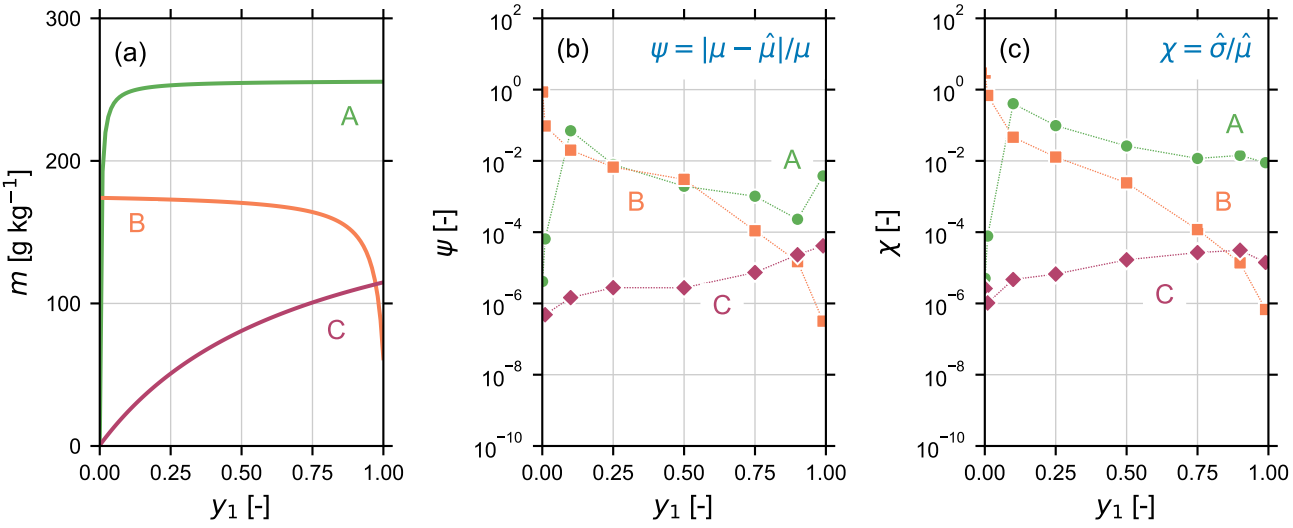

Figure 3: **(a)** Sensor response m, obtained using eq 2, for the three hypothetical arrays, each composed of one material for a two-gas system, as a function of the gas composition y_1. **(b)** The relative error of the estimated mean gas compositions ψ for the three hypothetical arrays as a function of the true gas composition. **(c)** The coefficient of variation χ for the three hypothetical arrays as a function of the true gas composition. Here, ψ and χ is computed by repeating the composition estimation for a 1000 iterations without accounting for measurement noise. Panel (b) and (c) is a semilog plot.

mixture. To this aim, the knee/elbow of the sensor response is found using an algorithm previously reported (Kneedle algorithm).[45] Here, the knee/elbow of the sensor response corresponds to the gas composition where the transition from a linear or nonlinear response to a saturated response or vice-versa occurs. This approach is qualitative and aims to rapidly eliminate materials or combination of materials that cannot resolve a gas mixture at a given composition. This method can also serve as a pre-screening step to reduce the number of materials that must be screened rigorously for constructing a sensor array (e.g. using the optimization methodology proposed previously[39]).

3.3.1 Two-Material Array

To illustrate the performance of the proposed methodology, we constructed two hypothetical arrays, D and E, using two materials each (α through δ). The sensor response for these two arrays are shown in Figure 4a,c. Using the Kneedle algorithm, the corresponding knee/elbow

was found. The algorithm provides the value of the gas composition where the transition in the sensor response occurs. Using this tool, we identified two regions for each material, namely, a more sensitive and a less sensitive regions. The former will encompass gas compositions that a material could resolve more accurately than the latter. The sensitive region for each material is highlighted as the shaded region (orange or green) in Figure 4a,c. For array D, exposure to a gas mixture with y_1 below 0.4 and for array E, exposure to a gas mixture with either y_1 below 0.1 or above 0.85 should yield a better performance when compared to other gas compositions.

Further, the approach used in Section 3.2 to quantify the relative error of the estimated mean composition ψ and the coefficient of variation χ, was employed for the two hypothetical arrays. These two quantities for arrays D and E, at different gas compositions is shown in Figure 4b and Figure 4d, respectively. Several observations can be made on the performance of both the arrays. Over the entire gas composition range, array D performs better than array E, indicated by lower ψ and χ values. For array D, while ψ does not change significantly, χ varies by an order of magnitude between the low and the high gas compositions. Additionally, the compositions that fall in the sensitive region (shaded region) have a lower value of χ. The difference in performance at different gas compositions are clearer for array E. The array performance is in line with the gas compositions that fall under the sensitive region, i.e. lower values of ψ and χ at both lower and high gas compositions. When outside the sensitive region, these quantities are 3-4 orders of magnitude higher than the best case scenario, highlighting the inability of the array to be used under conditions that have intermediate gas compositions. Finally, array D performs better than array E over the entire range of gas composition. Indeed, both materials in array D exhibit a change in the sensor response as the gas composition changes. For array E, at intermediate gas compositions, neither material γ nor δ exhibit any changes in sensor response.

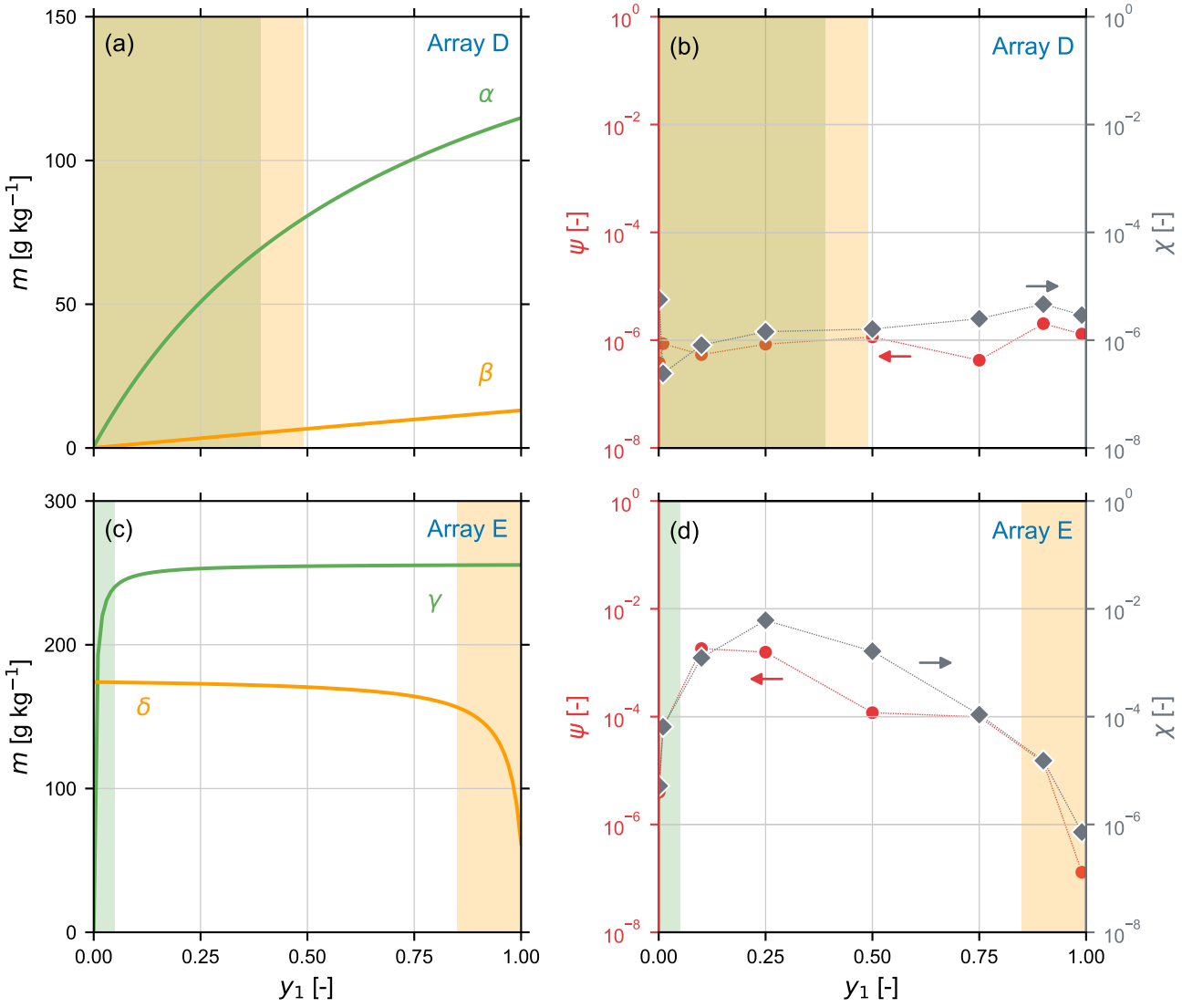

Figure 4: **(a)** Sensor response m, obtained using eq 2, for the hypothetical array D, composed of materials α and β for a two-gas system, as a function of the gas composition y_1. **(b)** The relative error of the estimated mean gas compositions ψ (red) and the coefficient of variation χ (gray) for the the hypothetical array D as a function of the true gas composition. **(c)** Sensor response m, obtained using eq 2, for the hypothetical array E, composed of materials γ and δ for a two-gas system, as a function of the gas composition y_1. **(d)** The relative error of the estimated mean gas compositions ψ (red) and the coefficient of variation χ (gray) for the hypothetical array E as a function of the true gas composition. Here, ψ and χ are computed by repeating the composition estimation for 1000 iterations without accounting for measurement noise. In panels (a) and (c), the shaded regions (orange and green) correspond to the sensitive region of the sensor response that would lead to a superior array performance. Panels (b) and (d) are semilog plots.

3.3.2 Three-Material Array

As shown in the previous subsection, the methodology proposed to identify the sensitive regions for the materials to resolve a gas mixture can describe the qualitative trends in the sensing performance for the two-material case. Here, we extended the methodology for a three-material array for two hypothetical arrays, F and G. The aim of this study is two-fold. First, to illustrate the ability of the methodology and explain the qualitative trends for a three-material array. Second, to illustrate the ability of the methodology to be used to mix and match materials to broaden the working range of the array.

For this study, we first constructed a reference two-material array using materials γ and ζ. Subsequently, we constructed the two hypothetical three-material arrays, F and G, by adding α and δ, respectively, to the reference array. The sensor response for these two arrays are shown in Figure 5a,c. Using the Kneedle algorithm, we identified the sensitive for each material in the array (shaded region in Figure 5a,c). The sensitive region for the reference two-material array covers the gas composition y_1 below 0.1. For array F, the sensitive region expands to y_1 of around 0.4 with the addition of material α. For array G, the sensitive region is concentrated on the two extremities of the gas composition by the addition of material δ.

Further, we employed the approach used in Section 3.2 to quantify the relative error of the estimated mean composition ψ and the coefficient of variation χ, for the reference array and the two hypothetical arrays, F and G. These two quantities are shown in Figure 5b and Figure 5d, for different gas compositions. The outcome from the study agrees with the two-material array scenario, discussed in the previous subsection. The reference two-material array performs best at gas compositions that fall within the sensitive region (y_1 below 0.10), indicated by the lower value of ψ and χ. As expected, the addition of a third material to the reference array enhances the performance by 3-4 orders of magnitude, when the composition of the test gas falls within the sensitive region. For array F, the addition of material α, improves the performance over the entire range of gas composition. This observation is

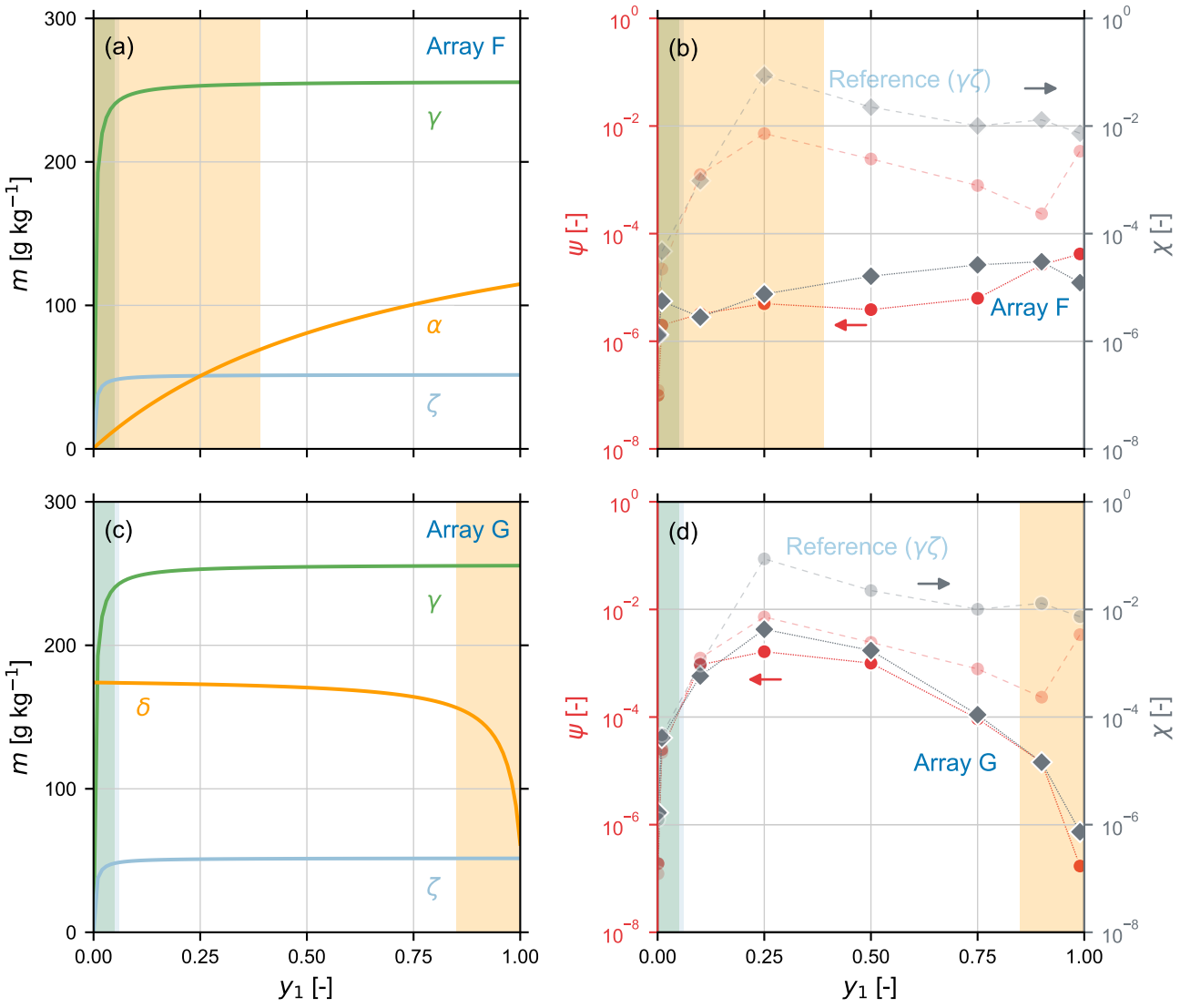

Figure 5: **(a)** Sensor response m, obtained using eq 2, for the hypothetical array F, composed of three materials γ, ζ, and α for a two-gas system, as a function of the gas composition y_1. **(b)** The relative error of the estimated mean gas compositions ψ (red) and the coefficient of variation χ (gray) for the the hypothetical array E and the reference array, composed of two materials γ and ζ, as a function of the true gas composition. **(c)** Sensor response m, obtained using eq 2, for the hypothetical array G, composed of three materials γ, ζ, and δ for a two gas system, as a function of the gas composition y_1. **(d)** The relative error of the estimated mean gas compositions ψ (red) and the coefficient of variation χ (gray) for the the hypothetical array G and the reference array, composed of two materials γ and ζ, as a function of the true gas composition. Here, ψ and χ are computed by repeating the composition estimation for a 1000 iterations without accounting for measurement noise. In panels (a) and (c), the shaded regions (green, blue, and orange) corresponds to the sensitive region of the sensor response that would lead to a superior array performance. Panels (b) and (d) are semilog plots

attributed to the shape of the response for material α (see discussion on array D). Array G performs better at both lower and higher compositions when compared to intermediate compositions (see discussion on array D). We attribute these observations to the shape of the sensor responses at the different gas compositions. Depending on the application of a given sensor array based on the target gas compositions, the reference array can be expanded by adding materials that would resolve the gas and the methodology proposed here could be used to rapidly evaluate if that is feasible. As a final comment, the addition of more materials to a sensor does not automatically guarantee an increase in performance. Instead, the gain in performance relies heavily on the sensitivity at a given target gas composition provided by the additional material.

To conclude, the studies presented on the two-material and three-material arrays reinforce the observations made in Section 3.2 regarding the impact of the nonlinearity (or shape) of the sensor response on the array performance. The studies also demonstrate the effectiveness of our methodology to use the knee/elbow of the sensor response as a proxy for the expected array performance under equilibrium conditions. The ability of the method to mix and match additional materials to improve the performance of a poor performing array is also observed using the three-material array. Overall, the methodology shown here can satisfactorily and quickly gauge the qualitative performance of a sensor array and to pre-screen materials before performing a rigorous optimization.

4 Thermodynamic and Kinetic Considerations

The observations from the previous section show that the thermodynamic/equilibrium characteristics of the materials in a sensor array determine its performance to accurately and consistently resolve a gas mixture. However, these studies were performed at equilibrium conditions. In practice, this assumption translates to a scenario where the kinetics of gas adsorption on the material is instantaneous (an equilibrium-controlled phenomenon). How-

ever, if gas adsorption is not instantaneous, one must incorporate the kinetics of the different gases in the material during the composition estimation and screening. The kinetics of the gas adsorption on the material will determine the response time of the sensor when subjected to a step-change in gas composition. A good sensor is one that has a very short response time, i.e. it should detect a change in gas composition, instantaneously.

When both thermodynamics and kinetics are incorporated, the sensing problem has a time-resolved mathematical formulation (see Section 2.1.3). This approach is closer to reality when compared to assuming an equilibrium sensing process. Additionally, this approach facilitates incorporating engineering variables like the size of the device (in terms of the volume) and the flow rate of the gas to be sensed, which is not possible with the equilibrium studies shown in the previous section or with the studies published previously.

In this section, we present a computational case study that highlights the need to employ a descriptive model incorporating adsorption kinetics, when the gas adsorption in a material is not instantaneous (Section 4.1). Subsequently, we simulate several scenarios to highlight the importance of factors like kinetics, flow rate of the gas and volume of the device on the sensing performance (Section 4.2).

4.1 Need to Employ a Descriptive Model

Here, we exposed the hypothetical array D to a binary gas mixture with inlet composition y_1^{in} of 0.1. The feed flow rate F_{in}, volume of the porous material V_{s}, and the dead volume of the device V_{g} were set to $5 \times 10^{-7}\text{m}^3\,\text{s}^{-1}$, $5 \times 10^{-7}\text{m}^3$, and $5 \times 10^{-7}\text{m}^3$, respectively. We assumed the same kinetic rate constant k of $0.01\,\text{s}^{-1}$ for all gases in all materials. We chose this low kinetic rate constant, which will lead to a very slow uptake, to highlight the necessity to consider kinetic effects when screening materials for sensor arrays and to reliably estimate the composition of the gas mixture.

The full model incorporating both the equilibrium and the kinetics, given by eq 6, is integrated for 1000 s to generate the "experimental" gas uptake profile $\mathbf{m}_{\text{exp},i}$ for each material

i in the array. This gas uptake profile for the hypothetical array D is shown in Figure 6a. Here, we can make two observations. First, due to the presence of adsorption kinetics, the sensor response m increases over time for both the materials. Second, after 750 s and 250 s, the response reaches a plateau for material α and β, respectively. This plateau corresponds to the equilibrium sensor response for both the materials. It is this equilibrium value that is used in all the screening studies reported in the literature. Depending on the kinetics of the gas in a given material, the response can plateau out sooner or later than the one shown here.

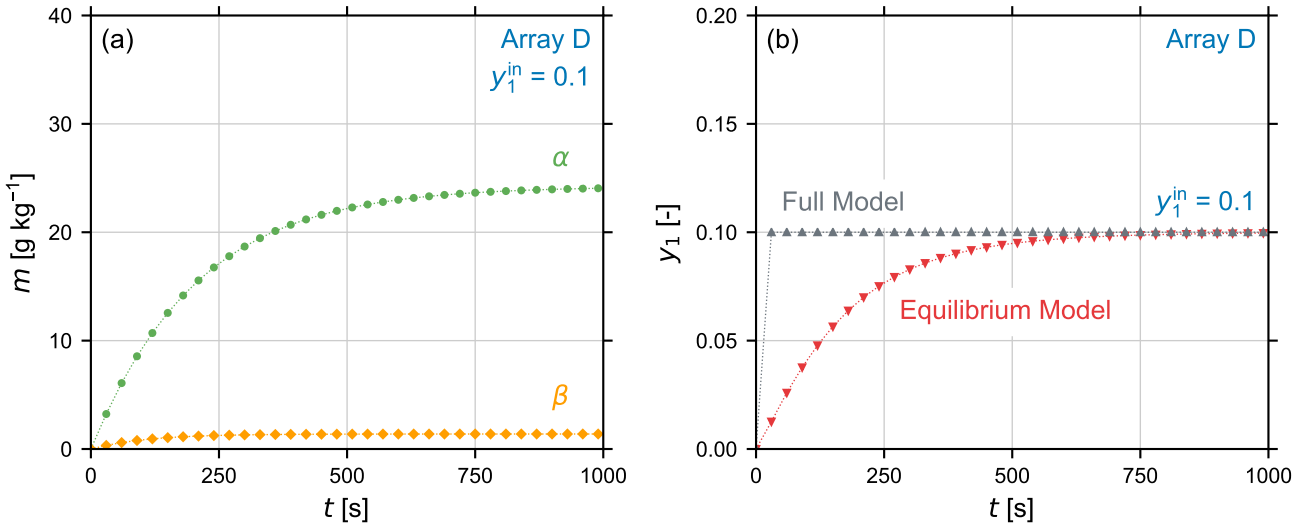

Figure 6: **(a)** Sensor response $\mathbf{m}_{exp}$, obtained using eq 6, for the hypothetical array D, composed of two materials α, and β for a two-gas system, as a function of time t for a feed gas composition y_1^{in} of 0.1. The response is generated using the same kinetic rate constant $k = 0.01\,s^{-1}$ for both the gases being sensed and both the materials used in the hypothetical array. **(b)** Estimated gas composition $\hat{y}_1$ as a function of time t obtained using a fully descriptive model (gray), given by eq 9, and using an equilibrium model (red), given by eq 8. Note: dotted lines serve only as a guide.

Given this sensor response, we considered two cases to estimate the binary mixture gas composition $\hat{y}_1$. In the first case, we estimated the gas composition without any knowledge of the adsorption kinetics, i.e. at each time instant, we assumed the gas to be at equilibrium with the porous material. Therefore, the optimization problem given by eq 8 is used to estimate the gas composition. In the second case, we estimated the gas composition with the

knowledge of adsorption kinetics, i.e. at each time instant, we considered both equilibrium and kinetic characteristics of the gas irrespective of whether the gas is at equilibrium or not. Therefore, we used the full model given by eq 6 and the optimization problem given by eq 9 to estimate the gas composition. The evolution of the gas compositions estimated using these two cases is shown in Figure 6b. Two observations can be made. First, the compositions estimated from the two cases differ and converge only after 750 s, in line with the plateau of the sensor response (see panel (a)). This is because the materials are at equilibrium with the feed gas at feed conditions after 750 s. Second, even though the sensor array is subjected to a feed gas at a constant composition, the equilibrium approach incorrectly predicts a variable feed gas composition. However, the full model, with the knowledge of both equilibrium and kinetics, resolves the composition accurately from the moment the array is exposed to the gas mixture.

To conclude, this simple case study highlights the importance of adsorption kinetics on gas sensing, an aspect that is often overlooked. Using a purely equilibrium approach for material screening and/or composition estimation is reasonable if the material reaches equilibrium rapidly. Since in practice, this might be difficult to achieve, one should either focus on using materials that exhibit minimal kinetic effects or on incorporating a detailed model for screening and/or composition estimation purposes in an array, like the one used in this work. Irrespective of the approach used, one must accurately characterize the kinetic characteristics apart from the equilibrium characteristics of a given material.

4.2 Factors that Impact Sensing Performance

The observations from the previous subsection show that kinetics impact significantly the sensing performance and the composition estimates thus obtained. However, when one looks at the detailed sensor model, given by eq 6, apart from the equilibrium (q^*) and kinetic (k) characteristics of the materials in the array, three other variables can potentially influence the sensing performance. These variables include: inlet gas volumetric flow rate F^{in}, dead

volume of the device V_g and volume of the porous material V_g coated on the sensor. The latter two variables can be defined using the total volume of the device V_T and the dead voidage of the device ϵ, i.e. $V_g = \epsilon V_T$ and $V_s = (1-\epsilon)V_T$. To understand the effect of these variables, we conducted a parametric study by varying k, F^{in}, V_T, or ϵ, one at a time, using the detailed sensor model eq 6. We conducted the study for a one-material array, array C, composed of material α when exposed to a feed gas of composition $y_1^{in} = 1.0$. Here, this simple case is considered to better highlight the interplay between the different variables. The impact of equilibrium characteristics has been discussed in detail in Section 3.

The detailed sensor model is integrated for 2000 s to generate the gas uptake profile $\mathbf{m}$ for the hypothetical array C. The gas uptake profile from varying the aforementioned four variables is shown in Figure 7. Several observations can be made from the outcome of this study. First, an increase in the kinetic rate constant k of gas being adsorbed decreases the time to reach the saturation uptake (see Figure 7a). Therefore, a higher value of k translates to a faster sensor response time when subjected to a step change in gas composition. Second, an increase in the gas volumetric flow rate F^{in} also decreases the time to reach the saturation uptake (see Figure 7b). A higher F^{in} ensures that the change in the sensor response is dictated purely by the kinetics of the adsorption and not by the convection of the gas. Third, an increase in the total volume of the device V_T at a constant dead voidage ϵ of the device increases the saturation uptake of the sensor (see Figure 7c). This is expected as an increase in V_T translates to a higher volume of the coated porous material V_s and thereby to a higher gas uptake. This feature might also help increase the signal-to-noise ratio of the sensor response when materials with low uptake are used in the array. Finally, an increase in the dead voidage of the device ϵ at a constant total volume of the device V_T, decreases the saturation uptake of the sensor (see Figure 7d). This is expected as an increase in ϵ translates to lower volume of coated porous material V_s.

To summarize, desirable characteristics for gas sensing include: material with fast kinetics (material constraint), a device that has a high total volume and a low dead voidage

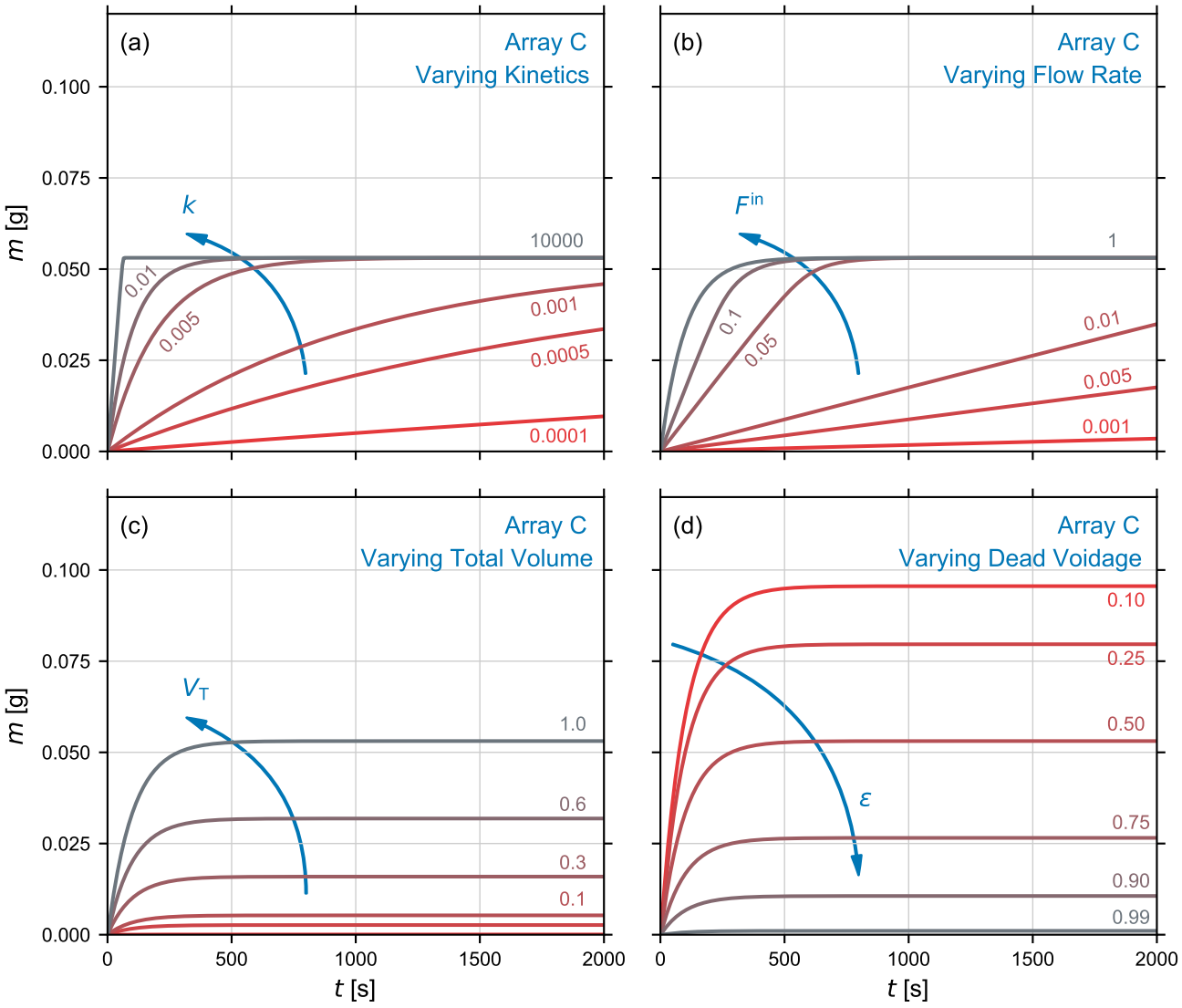

Figure 7: Sensor response **m**, obtained using eq 6, for the hypothetical array C, composed of material α for a two-gas system, as a function of time t for a feed gas composition y_1^{in} of 1.0. Response obtained from a parametric study by varying **(a)** kinetic rate constant k of the gases, **(b)** inlet gas volumetric flow rate F^{in}, **(c)** total volume of the device V_T (combined solid and gas phase) and **(d)** dead voidage of the device ϵ. The direction of the arrow indicates an increase in the variable being varied. The absolute amount absorbed is indicated in all the plots. The reference values of the variables are $k = 0.01$ s^{-1}, $F^{in} = 0.5$ $cm^3\,s^{-1}$, $V_T = 1$ cm^3 and $\epsilon = 0.5$. The value of the variables being varied in the corresponding parametric study, k [s^{-1}], F^{in} [$cm^3\,s^{-1}$], V_T [cm^3] and ϵ [-] is given in each panel.

additionally guaranteeing the ability to process a high flow rate of sensing gas (engineering constraints). In practice, one cannot arbitrarily set the values for these material and engineering variables. Therefore, a rigorous optimization has to be performed accounting for

realistic bounds of the variables before finalizing the design of the electronic nose. As a final comment, the observations seen here can have consequences when estimating the gas compositions of the gas to be sensed. If one incorporates a detailed sensor model, as discussed in Section 4.1, the gas composition can be estimated accurately irrespective of the choice of the variables. However, erroneous gas compositions are bound to be obtained when the composition estimation algorithm is blind to the effects of these variables, as in the case of the equilibrium model.

5 Concluding Remarks

5.1 Key Outcomes

The work presented here provides a new perspective into material screening for gas sensing applications. We present the first study that aims to systemically evaluate the effect of adsorption equilibrium (thermodynamics) and kinetics of the gas-material system on the performance of a gravimetric sensor array. To this aim, we have developed two computational tools. First, a sensor model, that incorporates either only the thermodynamics or a combination of both the thermodynamics and kinetics of the gas-material system. Second, a composition estimator coupled to the sensor model, to obtain the composition of the gases in the feed stream. The key outcomes from this work can be summarized as follows:

- One can exploit the shape of the sensor response as a function of gas composition to rapidly screen materials for gravimetric sensor arrays. This can serve as a prescreening tool to other screening approaches presented in the literature.

- One should incorporate both equilibrium and kinetics to accurately estimate gas compositions in a dynamic system.

- One should account for the gas flow rate, size of the device, and kinetics of the gas-material system, when screening materials as these variables can significantly impact

the sensor response.

Finally, the modeling framework and the methodology developed in this work is universal and is not restricted to any material/gas combination. If the sensing mechanism is based on gravimetry, this framework can be used to gauge the performance of any existing or new material combinations for a sensor array. Even though the results presented in this work are for a binary system, the methodology and the outcome are transferable to more than two gases.

5.2 Way forward

The accurate characterization of adsorption thermodynamics and kinetics of the materials has major implications not only on gas sensing using novel porous material like MOFs, but also on gas separation applications. Today, there are very few reports of multi-component adsorption equilibrium and even fewer studies on the kinetics of adsorption. If porous materials are to be used on scale for gas sensing applications, an accurate characterization is key. In our future work, we aim to address this knowledge gap by looking into sensing common gases on prototypical MOFs and characterizing the adsorption equilibrium and kinetic properties of the gas-material combination.

Supporting Information Available

The Python scripts for the sensor model and the concentration estimator will be made available upon publication of the article.

Acknowledgement

A.K.R. is thankful to the Swiss National Science Foundation for their financial support (Project Number 191875).

References

(1) Rodriguez-Mendez, M.; de Saja, J. A. *Advanced Nanomaterials for Inexpensive Gas Microsensors*; 2020; pp 37–54.

(2) Liu, X.; Cheng, S.; Liu, H.; Hu, S.; Zhang, D.; Ning, H. A Survey on Gas Sensing Technology. *Sensors* **2012**, *12*, 9635–9665.

(3) Aleixandre, M.; Gerboles, M. Review of small commercial sensors for indicative monitoring of ambient gas. *Chem. Eng. Trans.* **2012**, *30*, 169–174.

(4) Wagner, T.; Haffer, S.; Weinberger, C.; Klaus, D.; Tiemann, M. Mesoporous materials as gas sensors. *Chem. Soc. Rev.* **2013**, *42*, 4036–4053.

(5) Wales, D. J.; Grand, J.; Ting, V. P.; Burke, R. D.; Edler, K. J.; Bowen, C. R.; Mintova, S.; Burrows, A. D. Gas sensing using porous materials for automotive applications. *Chem. Soc. Rev.* **2015**, *44*, 4290–4321.

(6) Yi, F.-Y.; Chen, D.; Wu, M.-K.; Han, L.; Jiang, H.-L. Chemical Sensors Based on Metal-Organic Frameworks. *ChemPlusChem* **2016**, *81*, 675–690.

(7) Campbell, M.; Dincă, M. Metal-Organic Frameworks as Active Materials in Electronic Sensor Devices. *Sensors* **2017**, *17*, 1108.

(8) Stassen, I.; Burtch, N.; Talin, A.; Falcaro, P.; Allendorf, M.; Ameloot, R. An updated roadmap for the integration of metal-organic frameworks with electronic devices and chemical sensors. *Chem. Soc. Rev.* **2017**, *46*, 3185–3241.

(9) Devkota, J.; Kim, K. J.; Ohodnicki, P. R.; Culp, J. T.; Greve, D. W.; Lekse, J. W. Zeolitic imidazolate framework-coated acoustic sensors for room temperature detection of carbon dioxide and methane. *Nanoscale* **2018**, *10*, 8075–8087.

(10) Sumida, K.; Rogow, D. L.; Mason, J. A.; McDonald, T. M.; Bloch, E. D.; Herm, Z. R.; Bae, T.-H.; Long, J. R. Carbon Dioxide Capture in Metal-Organic Frameworks. *Chem. Rev.* **2012**, *112*, 724–781.

(11) Zhang, Z.; Yao, Z.-Z.; Xiang, S.; Chen, B. Perspective of microporous metal-organic frameworks for CO_2 capture and separation. *Energy Environ. Sci.* **2014**, *7*, 2868.

(12) Petit, C. Present and future of MOF research in the field of adsorption and molecular separation. *Curr. Opin. Chem. Eng.* **2018**, *20*, 132–142.

(13) Allendorf, M. D.; Houk, R. J. T.; Andruszkiewicz, L.; Talin, A. A.; Pikarsky, J.; Choudhury, A.; Gall, K. A.; Hesketh, P. J. Stress-Induced Chemical Detection Using Flexible Metal-Organic Frameworks. *J. Am. Chem. Soc.* **2008**, *130*, 14404–14405.

(14) Lu, G.; Hupp, J. T. Metal-Organic Frameworks as Sensors: A ZIF-8 Based Fabry-Pérot Device as a Selective Sensor for Chemical Vapors and Gases. *J. Am. Chem. Soc.* **2010**, *132*, 7832–7833.

(15) Campbell, M. G.; Liu, S. F.; Swager, T. M.; Dincă, M. Chemiresistive Sensor Arrays from Conductive 2D Metal-Organic Frameworks. *J. Am. Chem. Soc.* **2015**, *137*, 13780–13783.

(16) Yao, M.-S.; Tang, W.-X.; Wang, G.-E.; Nath, B.; Xu, G. MOF Thin Film-Coated Metal Oxide Nanowire Array: Significantly Improved Chemiresistor Sensor Performance. *Adv. Mater.* **2016**, *28*, 5229–5234.

(17) Ongari, D.; Liu, Y. M.; Smit, B. Can Metal–Organic Frameworks Be Used for Cannabis Breathalyzers? *ACS Appl. Mater. Interfaces* **2019**, *11*, 34777–34786.

(18) André, L.; Desbois, N.; Gros, C. P.; Brandès, S. Porous materials applied to biomarker sensing in exhaled breath for monitoring and detecting non-invasive pathologies. *Dalt. Trans.* **2020**, *49*, 15161–15170.

(19) Li, H.-Y.; Zhao, S.-N.; Zang, S.-Q.; Li, J. Functional metal–organic frameworks as effective sensors of gases and volatile compounds. *Chem. Soc. Rev.* **2020**, *49*, 6364–6401.

(20) Chappanda, K. N.; Shekhah, O.; Yassine, O.; Patole, S. P.; Eddaoudi, M.; Salama, K. N. The quest for highly sensitive QCM humidity sensors: The coating of CNT/MOF composite sensing films as case study. *Sensors Actuators B Chem.* **2018**, *257*, 609–619.

(21) Tchalala, M. R.; Belmabkhout, Y.; Adil, K.; Chappanda, K. N.; Cadiau, A.; Bhatt, P. M.; Salama, K. N.; Eddaoudi, M. Concurrent Sensing of CO_2 and H_2O from Air Using Ultramicroporous Fluorinated Metal-Organic Frameworks: Effect of Transduction Mechanism on the Sensing Performance. *ACS Appl. Mater. Interfaces* **2019**, *11*, 1706–1712.

(22) Gassensmith, J. J.; Kim, J. Y.; Holcroft, J. M.; Farha, O. K.; Stoddart, J. F.; Hupp, J. T.; Jeong, N. C. A Metal-Organic Framework-Based Material for Electrochemical Sensing of Carbon Dioxide. *J. Am. Chem. Soc.* **2014**, *136*, 8277–8282.

(23) Kim, K.-J.; Lu, P.; Culp, J. T.; Ohodnicki, P. R. Metal-Organic Framework Thin Film Coated Optical Fiber Sensors: A Novel Waveguide-Based Chemical Sensing Platform. *ACS Sensors* **2018**, *3*, 386–394.

(24) Dou, Z.; Yu, J.; Cui, Y.; Yang, Y.; Wang, Z.; Yang, D.; Qian, G. Luminescent Metal-Organic Framework Films As Highly Sensitive and Fast-Response Oxygen Sensors. *J. Am. Chem. Soc.* **2014**, *136*, 5527–5530.

(25) Wu, X.; Xiong, S.; Gong, Y.; Gong, Y.; Wu, W.; Mao, Z.; Liu, Q.; Hu, S.; Long, X. MOF-SMO hybrids as a H_2S sensor with superior sensitivity and selectivity. *Sensors Actuators B Chem.* **2019**, *292*, 32–39.

(26) Tchalala, M. R.; Bhatt, P. M.; Chappanda, K. N.; Tavares, S. R.; Adil, K.; Belmabkhout, Y.; Shkurenko, A.; Cadiau, A.; Heymans, N.; De Weireld, G.; Mau-

591 rin, G.; Salama, K. N.; Eddaoudi, M. Fluorinated MOF platform for selective removal
592 and sensing of SO_2 from flue gas and air. *Nat. Commun.* **2019**, *10*, 1328.

593 (27) Vashist, S. K.; Vashist, P. Recent Advances in Quartz Crystal Microbalance-Based
594 Sensors. *J. Sensors* **2011**, 1–13.

595 (28) Oprea, A.; Weimar, U. Gas sensors based on mass-sensitive transducers part 1: trans-
596 ducers and receptors—basic understanding. *Anal. Bioanal. Chem.* **2019**, *411*, 1761–
597 1787.

598 (29) Oprea, A.; Weimar, U. Gas sensors based on mass-sensitive transducers. Part 2: Im-
599 proving the sensors towards practical application. *Anal. Bioanal. Chem.* **2020**, *412*,
600 6707–6776.

601 (30) Dickinson, T. A.; White, J.; Kauer, J. S.; Walt, D. R. A chemical-detecting system
602 based on a cross-reactive optical sensor array. *Nature* **1996**, *382*, 697–700.

603 (31) Rakow, N. A.; Suslick, K. S. A colorimetric sensor array for odour visualization. *Nature*
604 **2000**, *406*, 710–713.

605 (32) Cho, J. H.; Kim, Y. W.; Na, K. J.; Jeon, G. J. Wireless electronic nose system for real-
606 time quantitative analysis of gas mixtures using micro-gas sensor array and neuro-fuzzy
607 network. *Sensors Actuators B Chem.* **2008**, *134*, 104–111.

608 (33) Chen, Z.; Zheng, Y.; Chen, K.; Li, H.; Jian, J. Concentration Estimator of Mixed VOC
609 Gases Using Sensor Array With Neural Networks and Decision Tree Learning. *IEEE*
610 *Sens. J.* **2017**, *17*, 1884–1892.

611 (34) Javed, U.; Ramaiyan, K. P.; Kreller, C. R.; Brosha, E. L.; Mukundan, R.; Moro-
612 zov, A. V. Using sensor arrays to decode $NO_x/NH_3/C_3H_8$ gas mixtures for automotive
613 exhaust monitoring. *Sensors Actuators B Chem.* **2018**, *264*, 110–118.

(35) Hu, W.; Wan, L.; Jian, Y.; Ren, C.; Jin, K.; Su, X.; Bai, X.; Haick, H.; Yao, M.; Wu, W. Electronic Noses: From Advanced Materials to Sensors Aided with Data Processing. *Adv. Mater. Technol.* **2018**, *4*, 1800488.

(36) Okur, S.; Zhang, Z.; Sarheed, M.; Nick, P.; Lemmer, U.; Heinke, L. Towards a MOF e-Nose: A SURMOF sensor array for detection and discrimination of plant oil scents and their mixtures. *Sensors Actuators B Chem.* **2020**, *306*, 127502.

(37) Gustafson, J. A.; Wilmer, C. E. Computational Design of Metal-Organic Framework Arrays for Gas Sensing: Influence of Array Size and Composition on Sensor Performance. *J. Phys. Chem. C* **2017**, *121*, 6033–6038.

(38) Gustafson, J. A.; Wilmer, C. E. Optimizing information content in MOF sensor arrays for analyzing methane-air mixtures. *Sensors Actuators B Chem.* **2018**, *267*, 483–493.

(39) Gustafson, J. A.; Wilmer, C. E. Intelligent Selection of Metal-Organic Framework Arrays for Methane Sensing via Genetic Algorithms. *ACS Sensors* **2019**, *4*, 1586–1593.

(40) Day, B. A.; Wilmer, C. E. Genetic Algorithm Design of MOF-based Gas Sensor Arrays for CO_2-in-Air Sensing. *Sensors* **2020**, *20*, 924.

(41) Sturluson, A.; Sousa, R.; Zhang, Y.; Huynh, M. T.; Laird, C.; York, A. H. P.; Silsby, C.; Chang, C.-H.; Simon, C. M. Curating Metal–Organic Frameworks To Compose Robust Gas Sensor Arrays in Dilute Conditions. *ACS Appl. Mater. Interfaces* **2020**, *12*, 6546–6564.

(42) Sousa, R.; Simon, C. M. Evaluating the Fitness of Combinations of Adsorbents for Quantitative Gas Sensor Arrays. *ACS Sensors* **2020**, *5*, 4035–4047.

(43) Brandani, S.; Mangano, E. The zero length column technique to measure adsorption equilibrium and kinetics: lessons learnt from 30 years of experience. *Adsorption* **2020**, *1*, 3.

(44) Virtanen, P. et al. SciPy 1.0: Fundamental Algorithms for Scientific Computing in Python. *Nature Methods* **2020**, *17*, 261–272.

(45) Satopaa, V.; Albrecht, J.; Irwin, D.; Raghavan, B. Finding a "Kneedle" in a Haystack: Detecting Knee Points in System Behavior. 2011 31st Int. Conf. Distrib. Comput. Syst. Work. 2011; pp 166–171.

Graphical TOC Entry: